Propagation of Gaussian Schell-model beams in modulated graded-index media

S. A. WADOOD,[1,2] **K. LIANG,**[1,2] **G. P. AGRAWAL,**[1,2,3] **T. D. VISSER,**[1,2,4] **C. R. STROUD JR.,**[1,2,3] **AND A. N. VAMIVAKAS**[1,2,3,5,*]

[1]*The Institute of Optics, University of Rochester, Rochester, New York 14627, USA*
[2]*Center for Coherence and Quantum Optics, University of Rochester, Rochester, New York 14627, USA*
[3]*Department of Physics and Astronomy, University of Rochester, Rochester, New York 14627, USA*
[4]*Department of Physics and Astronomy, Vrije Universiteit, Amsterdam, The Netherlands*
[5]*Materials Science, University of Rochester, Rochester, NY 14627, USA*
nick.vamivakas@rochester.edu

Abstract: The evolution of partially coherent beams in longitudinally modulated graded-index media is studied. The special cases of Gaussian Schell-model beams and parametric modulation, when the modulation period is half the fiber self-imaging period, are examined in detail. We show that the widths of the intensity and coherence of Gaussian Schell-model beams undergo amplification in parametrically modulated parabolic graded-index media. The process is an analog of quantum mechanical parametric amplification and generation of squeezed states. Our work may find application in spatial and temporal imaging of partially coherent beams in fiber-based imaging systems.

1. Introduction

Longitudinal modulation of optical waveguides is integral to photonic components such as filters, gratings, mode converters, and periodic polling in nonlinear optics [1]. The propagation of light in modulated waveguides is also of fundamental importance. Optical waveguides provide a test bed to construct optical analogs of diverse quantum effects such as coherent population transfer, Zeno dynamics, Bloch oscillations, and Anderson localization (see [2] for a review). In particular, the effect of harmonic modulation of optical waveguides on light propagation and localization has been extensively studied, and its connection to quantum mechanics elaborated [3,4].

With few exceptions [5,6], most of the works on modulated waveguides remain concerned with spatially coherent beams. The sources in nature, however, are partially coherent, and the subject of partial coherence is a field of its own [7]. Partial coherence is not always undesirable, as it has been proven to be robust against turbulent media [8]. It is therefore natural to extend the previous work to partially coherent beams. We can also ask what, if any, is the corresponding quantum mechanical analog?

We address these issues for the particular case of a parametrically modulated graded-index (GRIN) waveguide. We first show that the corresponding quantum mechanical analog for parametric modulation of such a waveguide is the degenerate parametric amplifier and the corresponding generation of squeezed states [7]. This connection, to the best of our knowledge, has not been made in the literature. We then show how partially coherent Gaussian Schell-model (GSM) beams evolve in parametrically modulated media. Two interesting features are shown: (1) The widths of the GSM beam's intensity (also referred to as spectral density) and coherence are parametrically amplified. (2) The beam undergoes self-imaging of intensity alongside the parametric amplification. Note that the energy of the beams is constant in our analysis, in contrast to the conventional *temporal* parametric amplification. It is only the width parameters of the beam that are amplified. Furthermore, we consider temporally coherent monochromatic beams in this work, and are concerned only with spatial coherence.

We consider GRIN media with a parabolic refractive index profile given by

$$n^2(x, z) = n_0^2 - a(z)x^2, \tag{1}$$

where $a(z)$ governs the longitudinal modulation of the parabolicity of the refractive index. The case of a constant $a(z) = a_0$ corresponds to the usual parabolic GRIN media. As is well known, the longitudinal propagation of a paraxial field in parabolic GRIN media is mathematically equivalent to the temporal evolution of a quantum harmonic oscillator's wave function in a quadratic potential [9,10]. The analogy has been used to analytically derive the propagation of fields and coherence functions through GRIN media. Ponomarenko [11] used the results of coherent state evolution to show that the CSD is self-imaged upon propagation in a parabolic GRIN medium with $a(z) = a_0$. Here we extend the results in [11] for a sinusoidal modulation of $a(z)$ at twice the 'spatial' frequency of the GRIN oscillator.

The paraxial wave equation for an optical field of amplitude $A(x, z) = \langle x|A(z)\rangle$ and wavelength λ_0 can be written as

$$i\partial_z|A\rangle = H(z)|A\rangle$$
$$= \left(\frac{p^2}{2m} + \frac{m\kappa^2(z)x^2}{2}\right)|A\rangle, \tag{2}$$

where $H(z)$ is the z dependent Hamiltonian, $m = k_0 = 2\pi/\lambda_0, p = -i\partial_x$, and $\kappa(z) = \sqrt{a(z)}/n_0$ is the longitudinal spatial frequency of the GRIN medium. Equation (2) is equivalent to the Schrödinger equation of a quantum harmonic oscillator with a time-dependent frequency $\omega(t)$, $\hbar = 1$, and z playing the role of time. For a parametrically driven oscillator, $a(z) = a_0(1 + \epsilon \sin(2\kappa_0 z + \theta_m))$. We impose the constraint $a(z) > 0$ so that the Hamiltonian has positive eigenvalues. Physically, this corresponds to an inverted parabolic refractive index profile which is necessary to guide a mode. The z evolution of the state is given by the unitary transformation $|A(z)\rangle = U(z)|A(0)\rangle$, where $U(z)$ satisfies the paraxial equation.

To set the stage, we first revisit important results for $\epsilon = 0$, $a(z) = a_0$. In this case, H in Eq. (2) is independent of z. Firstly, the eigenmodes are the Fock states i.e. the Hermite–Gauss (HG) beams. These beams remain invariant, upto a Gouy phase [12], upon propagation. Secondly, an initially coherent state $|A(0)\rangle = |\alpha_0\rangle$ evolves as $|A(z)\rangle = |\alpha_0 e^{-i\kappa_0 z}\rangle$, i.e., the state remains coherent upon evolution. The coherent states correspond to a set of complex Gaussian beams of width $\sigma = \sqrt{1/2m\kappa_0}$, with each beam characterized by an arbitrary position displacement and tilt phase, and the beam centroid exhibiting a sinusoidal motion with frequency $\kappa_0 = \sqrt{a_0}/n_0$. Finally, any arbitrary input field and coherence function will self-image with a period $\Lambda_0 = 2\pi/\kappa_0$ [11,13].

The general treatment for the case of time-dependent quadratic Hamiltonians such as given by Eq. (2) is a well-known problem, and has been treated in, for example, [14–17]. These works showed that time-dependent quadratic Hamiltonians lead to squeezing of input fields. In general, any Fock state evolves into a squeezed Fock state, and any coherent state evolves into a squeezed coherent state, also known as the two-photon coherent state [16]. The particular details of the squeezing are determined by the form of $\kappa(z)$. There are only a handful of systems for which there are closed form solutions. Among these, the most well-known is the parametric amplifier [7], the spatial analog of which we consider in this work.

The solution $|A(z)\rangle$ to Eq. (2) is found as follows. Using the harmonic oscillator ladder operators $a, a^\dagger$ such that $a = (ip + m\kappa_0 x)/\sqrt{2m\kappa_0}$, and writing $\kappa^2(z) = \kappa_0^2 \beta(z)$, the Hamiltonian in Eq. (2) can be recast into the form

$$H = \kappa_0[f_0(z)K_0 + f(z)K_+ + f^*(z)K_-], \tag{3}$$

where $K_0 = (a^\dagger a/2 + 1/4), K_+ = a^{\dagger 2}/2, K_- = a^2/2, f_0(z) = 1 + \beta(z)$, and $f(z) = [\beta(z) - 1]/2$. For the parametrically driven oscillator, we have $\beta(z) = 1 + \epsilon \sin(2\kappa_0 z + \theta_m)$. For this case, we have $f(z) = \epsilon \sin(2\kappa_0 z + \theta_m)/2$, and $f_0(z) = 2 + \epsilon \sin(2\kappa_0 z + \theta_m)$. We now make the so-called

rotating wave approximation (RWA). Note that the terms $e^{\pm i2\kappa_0 z}K_\pm$ are 'non-resonant' in Eq. (3). Similarly the term $\epsilon \sin(2\kappa_0 z)$ is non-resonant when multiplied with K_0. Using arguments from time-dependent perturbation theory, it can be shown that the contributions from the non-resonant terms are at least $1/\kappa_0$ times smaller than the resonant terms. Note that the difference in magnitude of resonant versus non-resonant effects is independent of the magnitude of ϵ. It is therefore an excellent approximation to ignore these terms, as is also verified by our simulations with the complete Hamiltonian of Eq. (3). Once these terms are ignored, then $f = i\epsilon \exp\left[-i(2\kappa_0 z + \theta_m)\right]/4$ and $f_0(z) = 2$. Under the RWA, the Hamiltonian then becomes

$$H = \kappa_0(a^\dagger a + 1/2) + \frac{i\kappa_0\epsilon}{4}[e^{-i(2\kappa_0 z + \theta_m)}K_+ - K_- e^{+i(2\kappa_0 z + \theta_m)}]$$
$$= H_0 + V,$$

(4)

where H_0 is the unperturbed harmonic oscillator Hamiltonian of frequency κ_0. The z evolution operator for the Hamiltonian in Eq. (4) can be written as [18]

$$U(z) = \exp[-i\kappa_0 z(a^\dagger a + 1/2)]\exp[\frac{\kappa_0 z\epsilon}{4}(K_+ e^{-i\theta_m} - K_- e^{i\theta_m})],$$
$$= \exp[-ih(z)K_0]\exp[\chi(z)K_+ - \chi^*(z)K_-],$$

(5)

where $h = 2\kappa_0 z$ and $\chi = (\kappa_0 z\epsilon/4)\exp(-i\theta_m)$.

We now explain the transverse structure of the field $A(x, z) = \langle x|A(z)\rangle = \langle x|U(z)|A(0)\rangle$. The squeeze operator $S(\chi) = \exp(\chi K_+ - \chi^* K_-)$ can be decomposed as $S(\chi) = e^{i\frac{\theta_\chi}{2}a^\dagger a}S(|\chi|)e^{-i\frac{\theta_\chi}{2}a^\dagger a}$ [19]. The operator $U(z)$ can then be written as

$$U(z) = e^{-i\frac{h-\theta_\chi}{2}(a^\dagger a + 1/2)}S(|\chi|)e^{-i\frac{\theta_\chi}{2}(a^\dagger a + 1/2)}.$$

(6)

Each factor on the right side of Eq. (6) has a distinct physical interpretation. The operator $\exp[-i\theta(a^\dagger a + 1/2)]$ corresponds to a fractional Fourier transform (frFt) such that $\langle x|\exp[-i\theta(a^\dagger a + 1/2)]||A\rangle$ is an frFt of order θ of the field $A(x)$. The operator $S(|\chi|)$ scales the field such that $\langle x|S(|\chi|)|A\rangle = e^{-|\chi|/2}A(e^{-|\chi|}x)$ [20]. The propagation is then a cascaded operation of an frFt of order $\theta_\chi/2$, a scaling by factor $|\chi|$, and an frFt of order $(h - \theta_\chi)/2$. Note that the propagation of the field in unmodulated GRIN media which have $a(z) = a_0, \chi = 0, h = 2\kappa_0 z$ corresponds to an frFt of order $\kappa_0 z$ in general [13]. Of course, the solution is valid only when the paraxial approximation holds.

2. Coherent field propagation

To propagate any arbitrary field, it is sufficient to have knowledge of propagation of modes forming a complete set. We therefore explicitly write out the propagated fields for the Fock states , i.e., the HG beams. Let an HG mode of order n be denoted by $\phi_n(x) = \langle x|n\rangle = \left(\frac{\sqrt{m\kappa_0/\pi}}{2^n n!}\right)^{1/2} H_n(\sqrt{m\kappa_0}x)e^{-m\kappa_0 x^2/2}$, where H_n denotes Hermite polynomials of order n, and $A(x, z = 0) = \phi_n(x)$. Then

$$A(x, z) = \langle x|U(z)|n\rangle = \langle x|e^{-i\frac{h-\theta_\chi}{2}(a^\dagger a + 1/2)}S(|\chi|)e^{-i\frac{\theta_\chi}{2}(a^\dagger a + 1/2)}|n\rangle,$$
$$= e^{-i\frac{\theta_\chi}{2}(n+1/2)}\langle x|e^{-i\frac{h-\theta_\chi}{2}(a^\dagger a + 1/2)}S(|\chi|)|n\rangle,$$

(7)

where we have used the property $e^{\theta a^\dagger a}|n\rangle = e^{\theta n}|n\rangle$, i.e., the HG beams are the eigenfunctions of the frFt. The function $\langle x|e^{-i\frac{h-\theta_\chi}{2}(a^\dagger a + 1/2)}S(|\chi|)|n\rangle$ is the frFt of order $(h - \theta_\chi)/2$ of the squeezed

function $e^{-|\chi|/2}\phi_n(e^{-|\chi|}x)$. Denoting $D = e^{-|\chi|}$, $B = (h - \theta_\chi)/2$, and using the scaling property of the frFt [21], we find

$$\langle x|e^{-iB(a^\dagger a+1/2)}S(|\chi|)|n\rangle = e^{-iC(n+1/2)}e^{i\Pi}\frac{\phi_n(\frac{Dx}{s})}{\sqrt{s/D}}, \tag{8}$$

$$A(x,z) = e^{-i(C+\frac{\theta_\chi}{2})(n+1/2)}e^{i\Pi}\frac{\phi_n(\frac{Dx}{s})}{\sqrt{s/D}}, \tag{9}$$

where $C = \arctan[D^2\tan(B)]$, $s = [1 + \sin^2(B)(D^4 - 1)]^{1/2}$, and $\Pi = m\kappa_0(\cot(C)/2)(s^2 - 1)(Dx/s)^2 = m\kappa_0\sin(2B)(D^4 - 1)(x/2s)^2$ is a z-dependent quadratic phase. Note that B, C, D, Π, s are all functions of z, and the factor of $(D/s)^{1/2}$ preserves the normalization of the squeezed HG mode $\phi_n(Dx/s)$.

Equation (9) has been previously derived in the context of squeezed Fock states [19,22]. In the context of GRIN media specifically, Eq. (9) shows that, like free space propagation, HG beams retain their general structure upon propagation in parametrically modulated GRIN media. The only quantities affected by any longitudinal refractive index modulation are the beam width and curvature. We stress the fact that such self-evolution of HG beams is true for arbitrary longitudinal modulation. The fact that Gaussian wavepackets retain their Gaussian structure in time-dependent quadratic potentials has been known since the beginning of Quantum Mechanics (see [23] and references therein), but has not been pointed out in the context of modulated parabolic GRIN waveguides to the best of our knowledge.

Figure 1 shows the Gaussian beam corresponding to the ground state wavefunction $\phi_0(x)$ evolving in a parametrically driven GRIN medium. We use the well known beam propagation method to propagate beams in GRIN media [24]. The algorithm consists of a cascade of free space
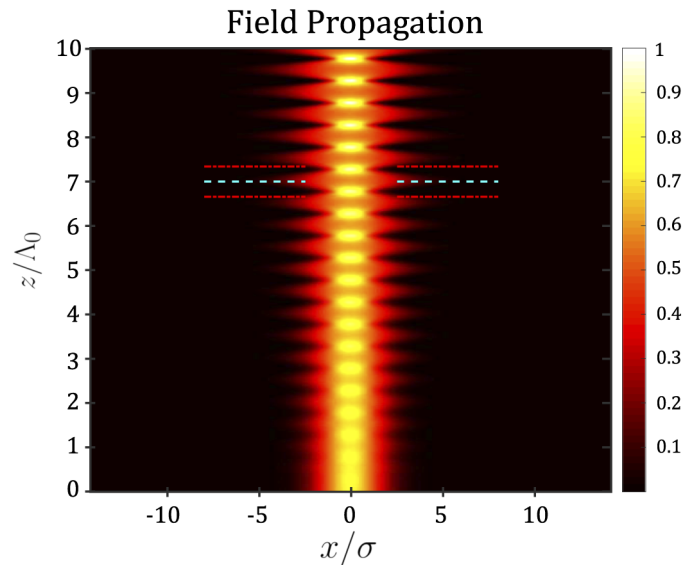

Fig. 1. Simulated amplitude of an input Gaussian mode ($A(x,0) = \langle x|0\rangle$) propagating through the parametrically modulated GRIN medium. The cyan dashed line indicates a location where the beam has no transverse quadratic phase, and also where the beam flips from being divergent to being convergent. The red dashed and dotted lines indicate locations where the beam intensity is equal to the input intensity, i.e., locations where the beam is self-imaged. The width of the beam is parametrically amplified.

propagation and lens focusing operations. The simulation parameters are : $\epsilon = 0.04$, $\theta_\chi = 0$, Total Z array size=1000, Total X array size=512, dx=0.25 μm, dz=0.01 Λ_0 where $\Lambda_0 = 2.4$ mm and $\lambda = 1$ μm. For the GRIN parameters we choose $n_0 = 1.47$, $a_0 = 2n_0^2\Delta/R^2$, where $\Delta = 0.0088$ is the index step and $R = 50$ μm is the fiber core radius. Even though the exact numbers are proprietary, these parameters are close to those of commercially available fibers [25]. Note that the self-imaging period $\Lambda_0 = 2.4$ mm implies a parametric modulation on a scale of $\Lambda_0/2 = 1.2$ mm. While they do not occur naturally in GRIN fibers, longitudinal refractive index modulations on a mm scale can be achieved, among other means, by i) modulating an applied stress on the fiber, ii) modulating the doping of the fiber core, and iii) using ultraviolet absorption techniques employed in the design of fiber gratings [26].

3. Gaussian Schell-model beam propagation

The beams considered so far were spatially coherent. We now extend our results to propagation of partially coherent beams. The evolution of partially coherent beams in unmodulated GRIN media ($\epsilon = 0$) is well known. We refer the reader to [27] for the treatment of GSM beams and to [11,28] for propagation of beams with arbitrary coherence properties through unmodulated GRIN media. In this section, we consider the specific class of extensively studied GSM beams propagating through parametrically modulated GRIN media.

Any partially coherent field is characterized by the Cross-Spectral Density (CSD) $W(x_1, x_2, z) = \langle A^*(x_1, z)A(x_2, z)\rangle$. The CSD for a GSM beam is given by

$$W(x_1, x_2, z = 0) = I_0 \exp\left[-(c + d)(x_1^2 + x_2^2) + 2dx_1x_2\right], \tag{10}$$

where I_0 is a positive constant, $c = 1/4\sigma_I^2$, and $d = 1/2\sigma_\mu^2$ such that the beam's intensity is $I(x) = W(x, x) = I_0 \exp\left(-x^2/2\sigma_I^2\right)$ and the spectral degree of coherence $\mu(x_1, x_2) = \exp\left[-(x_1^2 - x_2^2)/2\sigma_\mu^2\right]$ [29]. Note that the parameters c, d can depend on z, as will be shown later. The CSD can be expressed as an incoherent sum over individually coherent modes ψ_n [30] as

$$W(x_1, x_2, z) = \sum_n \lambda_n \psi_n^*(x_1, z)\psi_n(x_2, z), \tag{11}$$

where λ_n is the intensity in each mode, the set of modes ψ_n need not be complete or orthogonal in general, and the discrete sum over n can also be replaced by an integral in terms of a continuum of modes. The modes of the GSM beams can be found by solving the eigenvalue equation

$$\int dx_1 W(x_1, x_2, 0)\psi_n^*(x_1, 0) = \lambda_n \psi_n(x_2, 0), \tag{12}$$

where λ_n are the eigenvalues. An important result of coherence theory is that the modes $\psi_n(x)$ of a GSM source are scaled versions of the HG beams $\phi_n(x)$ with the eigenvalues given by

$$\lambda_n = I_0 \left(\frac{\pi}{c + d + q}\right)^{1/2} \left(\frac{d}{c + d + q}\right)^n, \tag{13}$$

and $q = (c^2 + 2cd)^{1/2}$ [29]. The modes $\psi_n(x) = r^{1/4}\phi_n(r^{1/2}x)$, where $r = 2q/m\kappa_0$, form a complete set. Note that when $q = m\kappa_0/2$, $r = 1$, and the GSM modes coincide exactly with the modes of the unmodulated GRIN medium. We can refer to this case as the CSD being 'mode-matched' to the GRIN medium. Note that using appropriate magnification optics with magnification factor of $\sqrt{r}$, any beam which is not mode-matched can be matched to a particular GRIN medium. We shall be concerned with mode-matched GRIN beams in our analysis. If the beam is not mode-matched, i.e., $r \neq 1$, the GSM modes are scaled versions of the Fock modes and therefore no longer eigenfunctions of the operator $a^\dagger a$. One cannot then in general replace the operator

$\exp(-i\theta_\chi a^\dagger a/2)$ with $\exp(-i\theta_\chi n/2)$ in Eq. (7), and the self-imaging property discussed below might not hold. There is, however, the special case of a real χ for which we can obtain an analytic solution by the replacement $\chi \to \chi + \sqrt{r}$ and the following results still hold.

For mode-matched GRIN beams, each coherent mode $\phi_n = \psi_n$ evolves according to Eqs. (7) and (9). In general, each mode acquires a quadratic phase Π as given in Eq. (9). By direct inspection of Eqs. (9) and (11), we see that the mode-matched GSM CSD evolves as

$$W(x_1, x_2, z) = \frac{D}{s} \sum_n \lambda_n e^{-i(\Pi_1 - \Pi_2)} \phi_n\left(\frac{Dx_1}{s}\right) \phi_n\left(\frac{Dx_2}{s}\right), \tag{14}$$

where Π_i is a function of x_i and z, and D, s are also functions of z, as explained after Eq. (9). In writing Eq. (14) we have used the fact that $\phi_n^* = \phi_n$. As expected from the coherent mode evolution in Eq. (9), we see that the longitudinal evolution of the CSD involves two features: i) scaling of the coherent modes by the factor D/s, and ii) accruing a quadratic phase $\Pi_1 - \Pi_2$. Due to the quadratic phase, the CSD in Eq. (14) is not strictly a scaled version of the input CSD given by Eq. (10). Nevertheless, we can draw some important general conclusions. The beam intensity remains Gaussian, while the width of the beam intensity varies longitudinally as $c(z) = c(0)D^2/s^2$, which implies $\sigma_I(z) = \sigma_I(0)s/D$. Similarly, the amplitude of the CSD, which does not depend on the phase Π, also varies according to $d(z) = d(0)D^2/s^2$, which implies $\sigma_\mu(z) = \sigma_\mu(0)s/D$. Therefore, the beam intensity and coherence functions retain their Gaussian form and their rms widths evolve simply by the factor of s/D. We now examine these findings in detail.

In certain conditions the quadratic phase can vanish, and then the CSD is an exact scaled version of the input CSD. Firstly, if we restrict ourselves to symmetric points about the GRIN axis such that $x_1 = -x_2$, the quadratic phase vanishes and we obtain the simple result $W(x, -x, z) = (D/s)W(Dx/s, -Dx/s, z = 0)$, i.e., the input CSD simply scales by the z-dependent factor D/s, and the factor of (D/s) upfront preserves normalization of the modes ϕ_n. Note that symmetric coherence functions are simpler to measure experimentally than the more general two-point CSD [31–33]. Secondly, there are locations z_0 where Π itself vanishes. For distances z_0 and an integer j such that $s = 1$, $2B = (2\kappa_0 z_0 - \theta_\chi) = j\pi$, the quadratic phase vanishes. Upto a global phase, the mode profile at z_0 is then given as $\phi_n(D_0 x)$, with $D_0 = \exp(-\kappa_0 \epsilon z_0/4)$. The CSD at z_0 is then given as

$$\begin{aligned} W(x_1, x_2, z = z_0) &= D_0 \sum_n \lambda_n \phi_n^*(D_0 x_1) \phi_n(D_0 x_2), \\ &= D_0 W(D_0 x_1, D_0 x_2, z = 0). \end{aligned} \tag{15}$$

which corresponds to a GSM beam with $c(z) = D_0^2 c(0)$, $d(z) = D_0^2 d(0)$. As explained above, the beam intensity and coherence functions retain their Gaussian form and their rms widths evolve under the envelopes described by $\sigma_I(z_0) = \sigma_I(0)\exp(\kappa_0 \epsilon z_0/4)$, $\sigma_\mu(z_0) = \sigma_\mu(0)\exp(\kappa_0 \epsilon z_0/4)$. The exponential growth of intensity width and coherence width is the spatial analog of the parametric amplification of a quantum state [34]. Note that the beam energy, which is proportional to $\int dx I(x, z)$, is invariant for all z because the dynamics are unitary. This is in contrast to the conventional *temporal* parametric amplification in which the beam energy increases exponentially over time. The analogy to quantum amplification applies only to the spatial intensity width and coherence widths of the beam. As an example, for a completely coherent beam as in Fig. 1, the cyan dashed line corresponds to $\kappa_0 z_0 = 7\pi$. Notice that the beam undergoes both focusing and expansion in Fig. 1.

Another interesting result is the phenomenon of self-imaging of intensity $I(x, z) = W(x, x, z)$. By self-imaging we mean the condition $I(x, 0) = I(x, z_i)$ for a particular z_i. This occurs whenever $D = s$, which corresponds to the solution of the transcendental equation $\exp(-2|\chi|) = 1 + \sin^2[(h - \theta_\chi)/2][\exp(-4|\chi|) - 1]$. For the Gaussian field propagation in Fig. 1, the different

z_i are marked by the blue circles in Fig. 2. Figure 2 shows the overlap integrals of the propagated complex field (amplitude) with the input complex field (amplitude). The field overlap gradually decreases, but there are revivals in the (absolute) amplitude overlap at each z_i. The small ripples in the field overlap simulations are the contributions from the non-resonant terms that were ignored in writing Eq. (4).
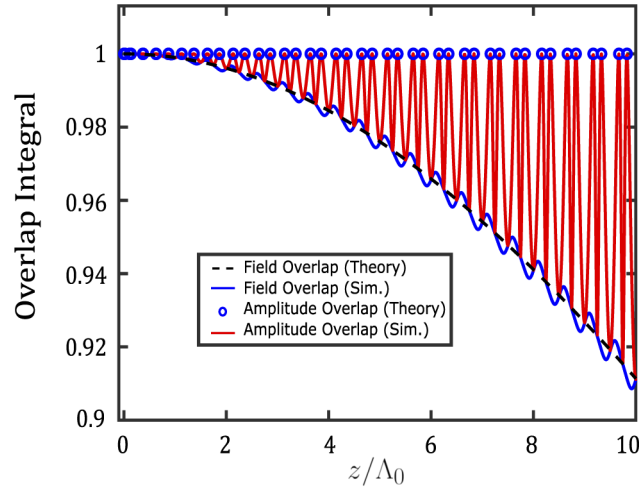

Fig. 2. (Dimensionless) Overlap integral for the input field $\left[\left| \int dx A^*(x,z) A(x,0) \right| \right]$ and amplitude $\left[\int dx |A(x,z)| |A(x,0)| \right]$ as a function of z/Λ_0 where $\Lambda_0 = 2.4$ mm is the spatial period associated with the GRIN oscillator. The simulated results are derived from the propagated Gaussian field shown in Fig. 1. The dashed black line shows the theoretically expected overlap integral for the field, while the solid blue line shows the corresponding results for the simulation. The blue circles show theoretically expected points of self-imaging of intensity, while the solid red line shows the intensity overlap calculated for the simulated Gaussian beam in Fig. 1. Note also that by choice we use a field amplitude overlap metric instead of the intensity overlap metric because the former is bounded above by unity while the latter has an upper bound greater than unity, i.e., it is possible to have $\int dx\, I^2(x,z) > 1$. For the simulated results, the overlap integral has been normalized to the maximum value, which also occurs at the input plane $z = 0$.

A mode-matched GSM beam can be characterized by the factor $\eta = \sigma_\mu/\sigma_I$, which characterizes the 'degree of global coherence' of a beam [29]. The limits $\eta \to 0, \infty$ correspond to completely spatially incoherent and coherent fields respectively. Note that for a mode-matched beam each η maps to a unique σ_I, and the two are related as

$$\sigma_I = \frac{1}{\sqrt{2m\kappa}} \left(1 + \frac{4}{\eta^2} \right)^{1/4}. \tag{16}$$

Figure 3 shows the evolution of intensity of GSM beams with different η values. Qualitatively, all the beams evolve in a similar fashion. Each beam experiences periodic focusing and defocusing, with the widths being parametrically amplified. Also, as shown for the coherent field in Fig. 2, there are locations z_i where the intensity self images. Physically, these are the locations between a focusing and expansion of the beam where the beam width equals the input beam width. Note that z_i only depends on the GRIN parameters, and not on the beam parameters. More importantly, $\eta(z) = \sigma_\mu(z)/\sigma_I(z)$ remains invariant, a feature also shared by free space propagation of GSM beams [7, Eq. 5.6-109].
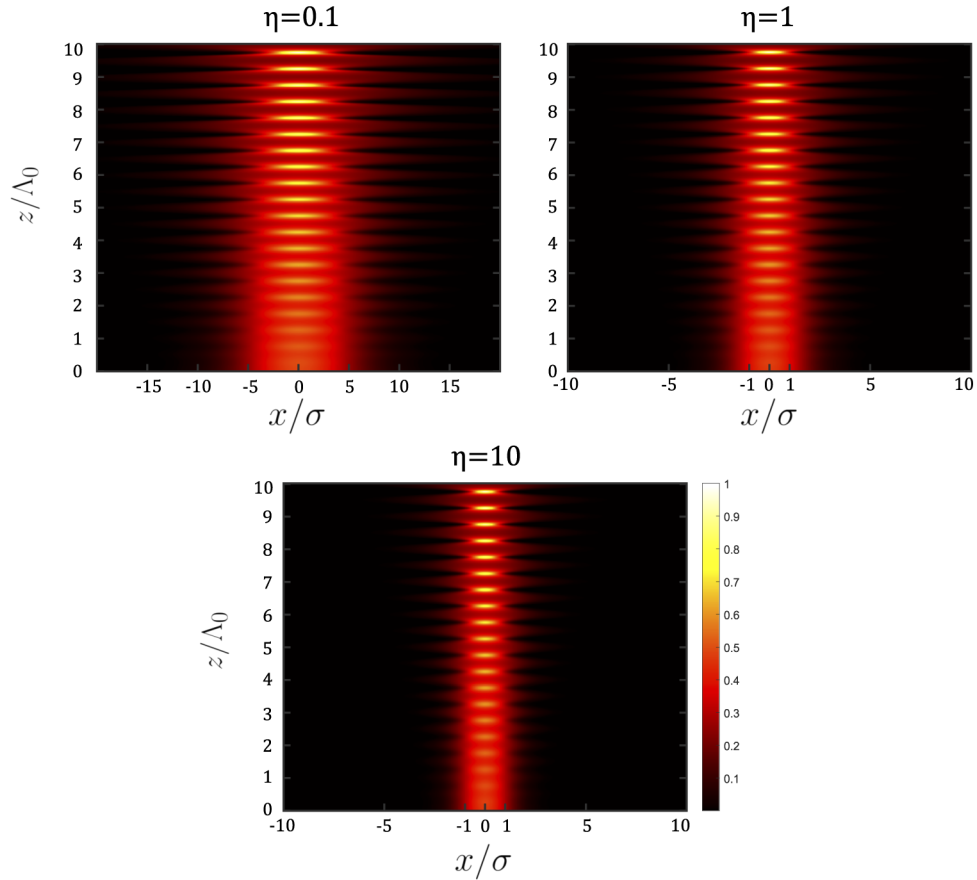
Fig. 3. Spectral Density propagation for GSM beams with different η parameters. The input beam is assumed to be mode matched and therefore the more incoherent the beam (smaller η), the wider the beam width. All beams exhibit the exponential amplification of beam width and self imaging of intensity as depicted in Fig. 2. For these figures, $\epsilon = 0.05$ and X array size=1024. The rest of the parameters are the same as used in Fig. 1.

Figure 4 shows the evolution of the second moment $\langle \Delta x^2(z) \rangle = \int dx x^2 I(x, z)$ of a GSM beam with $\eta = 0.5$. The solid red line plots the numerically computed ratio $\langle \Delta x^2(z) \rangle / \langle \Delta x^2(0) \rangle$. The blue lines are the envelopes given by $D^{\pm 2} = \exp(\mp \kappa_0 \epsilon z_0 / 2)$. The exponential growth is due to parametric modulation of the refractive index. The oscillation of the beam width is due to the focusing and expansion of the beam in the GRIN medium, and is given simply by the factor of $(s/D)^2$. Note that s/D has a quasi-spatial frequency of $2\kappa_0$, which is also the frequency of the parametric drive $a(z)$. As shown in Fig. 4, this means that, apart from the width amplification and suppression, the beam expands and focuses every $\Lambda_0/2$. In the quantum mechanical analogy, it would be the variance of the quadrature $(a + a^\dagger)$ that would be parametrically amplified [7, Chap. 22], and the dashed blue line is the analog of the effective 'vacuum' noise of the field mode. The focusing of the beam width below the dashed blue line is the analog of generating a 'temporal' squeezed state [7, Chap. 21]. Care must be taken, however, when making these analogies. The analogy is mathematically exact because the Hamiltonian in Eq. (4) has the same form as a temporal parametric amplifier. However, the mechanism to generate the parametric modulation can correspond to different physical processes in each case. While in the GRIN medium the refractive index is modulated longitudinally in space, the temporal parametric

amplifier uses nonlinear interaction between electric fields to generate a time-varying polarization in the medium. The former is a linear optics problem, while the latter falls in the domain of nonlinear optics. Another feature expressed in Fig. 4 is the self-imaging of the beam. When the solid red line crosses the dashed blue line, $\langle \Delta x^2(z) \rangle = \langle \Delta x^2(0) \rangle$ and the beam self images. These are precisely the locations z_i, also discussed in Fig. 2. Notice that the lower envelope $\exp(-\kappa_0 \epsilon z_0/2)$ shows that the beam focus also becomes narrower with propagation, a feature that might find application in fiber-based imaging systems. A similar result was also reported in [5], although using a slightly different approach based on Green's functions. Recall, however, that our results are valid under the paraxial approximation. At some point the paraxial approximation will break down because the diffraction angles required by the beam to expand and focus within $\Lambda_0/2$ increase with propagation.
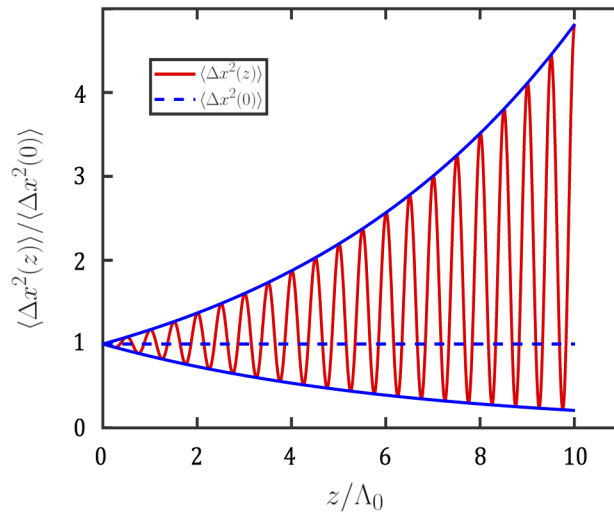

Fig. 4. Longitudinal evolution of beam width for a mode-matched input GSM beam with $\eta = 0.5$. The solid red line denotes the simulation results for the ratio $\langle \Delta x^2(z) \rangle / \langle \Delta x^2(0) \rangle$, where $\langle \Delta x^2(z) \rangle = \int dx x^2 I(x, z)$ is the transverse beam width at z, and $\langle \Delta x^2(0) \rangle$ is the input beam width. The dashed blue line denotes the input beam width level. The solid blue lines are theoretical envelopes $\exp[\pm \kappa_0 \epsilon z_0/2]$. The beam width is parametrically amplified as shown by the exponential envelopes. As explained in the text, this parametric amplification is mathematically analogous to the quantum mechanical amplification of the photon number in a conventional parametric amplifier. The phase of the beam width oscillations is controlled by θ_m, the phase of the longitudinal refractive index modulation. For this figure, we set $\theta_m = 0$. The beam is self-imaged at the locations where the solid red line crosses the dashed blue line, see Fig. 2. All simulation parameters are the same as used for Fig. 3.

4. Beam displacement and tilt: centroid amplification

The previous results of coherence width amplification and self-imaging assumed the input beam to be normally incident and centered on the input face of the GRIN medium. If the input GSM beam is displaced from the GRIN core or strikes at an angle, the beam centroid is parametrically amplified upon propagation. Beam centroid amplification has been observed in spatial solitons [35]. A coherent mode $\phi_n(x)$ that is displaced in position by x_0 and in momentum by p_0 is characterized by a complex parameter $\alpha = (ip_0 + m\kappa_0 x_0)/(2m\kappa_0)^{(1/2)}$ such that $|\alpha, n\rangle = D(\alpha)|n\rangle$, where $D(\alpha) = \exp(\alpha a^\dagger - \alpha^* a)$ is the displacement operator. The states $|\alpha, n\rangle$ are also referred to as displaced Fock states [22]. Similar to the derivation leading to Eq. (9), we find the expression

for $\langle x|U(z)|\alpha\rangle$, given the initial state $A(x, z = 0) = \langle x|\alpha, n\rangle$ as

$$
\begin{aligned}
A(x, z) = \langle x|U(z)|\alpha, n\rangle &= \langle x|e^{-i\frac{h}{4}}e^{-i\frac{h}{2}a^\dagger a}S(\chi)D(\alpha)|n\rangle, \\
&= e^{-i\frac{h}{4}}\langle x|e^{-i\frac{h}{2}a^\dagger a}D(\alpha')e^{+i\frac{h}{2}a^\dagger a}e^{-i\frac{h}{2}a^\dagger a}S(\chi)|n\rangle, \\
&= e^{-i\frac{h}{4}}\langle x|D(\alpha'e^{i\frac{h}{2}})e^{-i\frac{h}{2}a^\dagger a}S(\chi)|n\rangle.
\end{aligned}
\tag{17}
$$

In deriving Eq. (17), we have used the relation $S(\chi)D(\alpha) = D(\alpha')S(\chi)$, where $\alpha' = \mu\alpha + \nu\alpha^*$, $\mu = \cosh(|\chi|)$, $\nu = \sinh(|\chi|)e^{i\arg(\chi)}$. We also used the relation $e^{-i\theta a^\dagger a}D(\alpha)e^{i\theta a^\dagger a} = D(\alpha e^{i\theta})$. Finally, we can use the relation $\langle x|D(\alpha)|\Psi\rangle = e^{-i\text{Im}(\alpha)\text{Re}(\alpha)}e^{i\sqrt{2m\kappa_0}\text{Im}(\alpha)x}\Psi\left(x - \frac{\text{Re}(\alpha)}{\sqrt{m\kappa/2}}\right)$, that shows how $D(\alpha)$ shifts a function and adds a linear tilt phase, to write $A(x, z)$ as

$$
A(x, z) = e^{-i\text{Im}(\tilde{\alpha})\text{Re}(\tilde{\alpha})}e^{i\sqrt{2m\kappa_0}\text{Im}(\tilde{\alpha})x}\langle x - x_t|U(z)|n\rangle,
\tag{18}
$$

where $\tilde{\alpha} = \alpha'e^{i\frac{h}{2}}$, $x_t = \frac{\text{Re}(\tilde{\alpha})}{\sqrt{m\kappa/2}}$, and $\langle x|U(z)|n\rangle$ is found from Eqs. (7) and (9). For example, if the beam is normally incident, $p_0 = 0$, and displaced in position by x_0, then x_t is given as

$$
x_t = x_0\left[\cosh(\kappa_0\epsilon z/4)\cos(\kappa_0 z) + \sinh(\kappa_0\epsilon z/4)\cos(\kappa_0 z + \theta_m)\right].
\tag{19}
$$

We can now write the CSD for input GSM beams displaced by the complex parameter α, as

$$
\begin{aligned}
W(x_1, x_2, z, \alpha) &= e^{-i\sqrt{2m\kappa_0}\text{Im}(\tilde{\alpha})(x_2 - x_1)}\sum_n \lambda_n\langle x_1 - x_t|U(z)|n\rangle\langle n|U(z)|x_2 - x_t\rangle, \\
&= e^{-i\sqrt{2m\kappa_0}\text{Im}(\tilde{\alpha})(x_2 - x_1)}\sum_n \lambda_n\phi_n(x_1 - x_t, z)\phi_n^*(x_2 - x_t, z), \\
&= e^{-i\sqrt{2m\kappa_0}\text{Im}(\tilde{\alpha})(x_2 - x_1)}W(x_1 - x_t, x_2 - x_t, z, \alpha = 0),
\end{aligned}
\tag{20}
$$

where $W(x_1, x_2, z, \alpha = 0)$ corresponds to the propagated CSD with no input displacement in position or momentum. The intensity for the displaced GSM beams is also displaced by x_t, while the spectral degree of coherence still depends on $(x_2 - x_1)$. There is an extra tilt phase $\exp[-i\sqrt{2m\kappa_0}\text{Im}(\tilde{\alpha})(x_2 - x_1)]$ added to the CSD. The general observations for $z = z_0$ made in Eq. (15) still hold. At $z = z_0$, we have

$$
W(x_1, x_2, z_0, \alpha) = e^{-i\sqrt{2m\kappa_0}\text{Im}(\tilde{\alpha})(x_2 - x_1)}D_0 W\left(D_0(x_1 - x_t), D_0(x_2 - x_t), z = 0, \alpha = 0\right),
\tag{21}
$$

and the intensity and coherence rms widths still grow exponentially with the envelopes $\exp(\pm\kappa_0\epsilon z_0/4)$ while maintaining a constant global degree of coherence. Figure 5(a) shows the intensity evolution of a zeroth order Gaussian mode $\phi_0(x)$ which is displaced by 0.27σ at the fiber input. The centroid evolution of the beam is depicted in Figs. 5(b) and (c) for $\theta_m = 0, \pi$ respectively; these figures show phase-sensitive centroid amplification or suppression as predicted by Eq. (19).

Many features of our work such as mode matching and beam focusing share similarities with the work done in [5,6]. Our results could, in principle, be derived from the analysis in these papers, which solve the general problem of propagation of partially coherent beams in longitudinally modulated GRIN media. In our work we examine in detail the special case of a parametric modulation, which was not the focus of these previous works. To the best of our knowledge, we are not aware of any other works that show the i) the connection to the squeezing Hamiltonian of quantum mechanics to parametrically modulated GRIN media, and the corresponding parametric amplification of the intensity and coherence widths, ii) the use of the CMD for the GSM beam propagation in longitudinally modulated GRIN media.
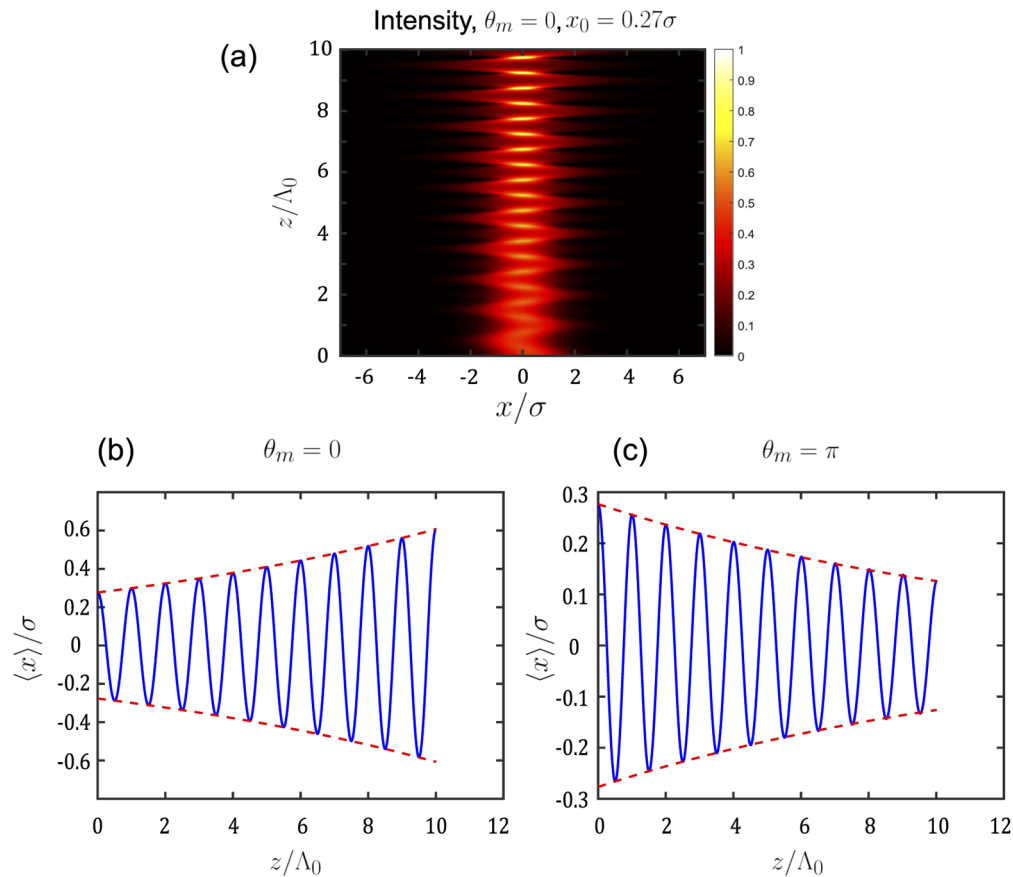
Fig. 5. (a) Centroid amplification of an input Gaussian mode which is displaced from the optical axis by 0.27σ. The centroid amplification is sensitive to the pump phase θ_m. (b) Simulated centroid (solid blue line) of the beam in (a), and the envelope (dashed red line) predicted by Eq. (19) for $\theta_m = 0$. (c) Centroid evolution for $\theta_m = \pi$. All other simulation parameters are same as in Fig. 3.

5. Conclusion

In summary, using results from quantum theory of parametric amplifiers we have shown the amplification of intensity width and coherence width of GSM beams in parametrically modulated GRIN media. We also show that self-imaging of GSM beams still occurs alongside amplification. Moreover, the degree of global coherence is invariant upon propagation, a feature shared by GSM beams in free space. Our results can be used in fiber-based imaging systems, and also to study quantum statistics of squeezed states in an optical analog setting. Our analysis can be extended to the time domain, and employed in temporal imaging with partially coherent pulses. Specifically, our work can be extended to partially coherent temporal GSM pulses propagating in 'temporal' GRIN media, i.e., nonlinear dispersive fibers [36]. There, the temporal coherence function would be amplified and the pulse would also show self-imaging.

Disclosures. The authors declare that there are no conflicts of interest related to this article.

Data availability. No data were generated for this paper. The codes for the simulation can be obtained from the authors upon reasonable request.

References

1. B. E. Saleh and M. C. Teich, *Fundamentals of photonics* (John Wiley & Sons, 2019).
2. S. Longhi, "Quantum-optical analogies using photonic structures," Laser Photonics Rev. **3**(3), 243–261 (2009).
3. A. Alberucci, L. Marrucci, and G. Assanto, "Light confinement via periodic modulation of the refractive index," New J. Phys. **15**(8), 083013 (2013).
4. I. L. Garanovich, S. Longhi, A. A. Sukhorukov, and Y. S. Kivshar, "Light propagation and localization in modulated photonic lattices and waveguides," Phys. Rep. **518**(1-2), 1–79 (2012).
5. S. Krivoshlykov, N. I. Petrov, and I. Sisakyan, "Spatial coherence of optical fields in longitudinally inhomogeneous media with quadratic refractive index profiles," Sov. J. Quantum Electron. **15**(3), 330–338 (1985).
6. S. Krivoshlykov, N. Petrov, and I. Sissakian, "Density-matrix formalism for partially coherent optical fields propagating in slightly inhomogeneous media," Opt. Quantum Electron. **18**(4), 253–264 (1986).
7. L. Mandel and E. Wolf, *Optical Coherence and Quantum Optics* (Cambridge university press, 1995).
8. S. Ponomarenko, J.-J. Greffet, and E. Wolf, "The diffusion of partially coherent beams in turbulent media," Opt. Commun. **208**(1-3), 1–8 (2002).
9. D. Gloge and D. Marcuse, "Formal quantum theory of light rays," J. Opt. Soc. Am. **59**(12), 1629–1631 (1969).
10. M. A. Marte and S. Stenholm, "Paraxial light and atom optics: the optical schrödinger equation and beyond," Phys. Rev. A **56**(4), 2940–2953 (1997).
11. S. A. Ponomarenko, "Self-imaging of partially coherent light in graded-index media," Opt. Lett. **40**(4), 566–568 (2015).
12. S. Van Enk and G. Nienhuis, "Eigenfunction description of laser beams and orbital angular momentum of light," Opt. Commun. **94**(1-3), 147–158 (1992).
13. D. Mendlovic and H. M. Ozaktas, "Fractional fourier transforms and their optical implementation: I," J. Opt. Soc. Am. A **10**(9), 1875–1881 (1993).
14. H. R. Lewis Jr and W. Riesenfeld, "An exact quantum theory of the time-dependent harmonic oscillator and of a charged particle in a time-dependent electromagnetic field," J. Math. Phys. **10**(8), 1458–1473 (1969).
15. E. J. Heller, "Time-dependent approach to semiclassical dynamics," J. Chem. Phys. **62**(4), 1544–1555 (1975).
16. H. P. Yuen, "Two-photon coherent states of the radiation field," Phys. Rev. A **13**(6), 2226–2243 (1976).
17. J. M. Cervero and J. D. Lejarreta, "SO (2, 1) invariant systems: squeezing and topological phases," Quantum Opt. **2**(5), 333–349 (1990).
18. C. C. Gerry, "Application of SU (1, 1) coherent states to the interaction of squeezed light in an anharmonic oscillator," Phys. Rev. A **35**(5), 2146–2149 (1987).
19. K. Mo, T. Jo, and J. P. Dahl, "Displaced squeezed number states: Position space representation, inner product, and some applications," Phys. Rev. A **54**(6), 5378–5385 (1996).
20. M. M. Nieto, "Functional forms for the squeeze and the time-displacement operators," Quantum Semiclassical Opt. **8**(5), 1061–1066 (1996).
21. A. W. Lohmann, Z. Zalevsky, R. G. Dorsch, and D. Mendlovic, "Experimental considerations and scaling property of the fractional fourier transform," Opt. Commun. **146**(1-6), 55–61 (1998).
22. P. Král, "Displaced and squeezed fock states," J. Mod. Opt. **37**(5), 889–917 (1990).
23. M. Andrews, "Invariant operators for quadratic hamiltonians," Am. J. Phys. **67**(4), 336–343 (1999).
24. M. Feit and J. Fleck, "Light propagation in graded-index optical fibers," Appl. Opt. **17**(24), 3990–3998 (1978).
25. M. Conforti, C. M. Arabi, A. Mussot, and A. Kudlinski, "Fast and accurate modeling of nonlinear pulse propagation in graded-index multimode fibers," Opt. Lett. **42**(19), 4004–4007 (2017).
26. R. Kashyap, *Fiber Bragg Gratings* (Academic press, 2009).
27. H. Roychowdhury, G. P. Agrawal, and E. Wolf, "Changes in the spectrum, in the spectral degree of polarization, and in the spectral degree of coherence of a partially coherent beam propagating through a gradient-index fiber," J. Opt. Soc. Am. A **23**(4), 940–948 (2006).
28. G. Agrawal, A. Ghatak, and C. Mehta, "Propagation of a partially coherent beam through selfoc fibers," Opt. Commun. **12**(3), 333–337 (1974).
29. A. Starikov and E. Wolf, "Coherent-mode representation of Gaussian Schell-model sources and of their radiation fields," J. Opt. Soc. Am. **72**(7), 923–928 (1982).
30. E. Wolf, "New spectral representation of random sources and of the partially coherent fields that they generate," Opt. Commun. **38**(1), 3–6 (1981).
31. J. B. Breckinridge, "Coherence interferometer and astronomical applications," Appl. Opt. **11**(12), 2996_1 (1972).
32. M. Santarsiero and R. Borghi, "Measuring spatial coherence by using a reversed-wavefront young interferometer," Opt. Lett. **31**(7), 861–863 (2006).
33. D. P. Brown and T. G. Brown, "Partially correlated azimuthal vortex illumination: coherence and correlation measurements and effects in imaging," Opt. Express **16**(25), 20418–20426 (2008).
34. B. Mollow and R. Glauber, "Quantum theory of parametric amplification. i," Phys. Rev. **160**(5), 1076–1096 (1967).
35. Y. V. Kartashov, L. Torner, and V. A. Vysloukh, "Parametric amplification of soliton steering in optical lattices," Opt. Lett. **29**(10), 1102–1104 (2004).
36. F. J. Marinho and L. M. Bernardo, "Graded-index time-lens implementation," Opt. Lett. **31**(11), 1723–1725 (2006).